Ocean Science

Relating Agulhas leakage to the Agulhas Current retroflection location

E. van Sebille[1], C. N. Barron[2], A. Biastoch[3], P. J. van Leeuwen[1,*], F. C. Vossepoel[1,4,], and W. P. M. de Ruijter[1]**

[1]Institute for Marine and Atmospheric Research Utrecht, Utrecht University, The Netherlands
[2]Naval Research Laboratory, Stennis Space Center, Mississippi, USA
[3]Leibniz Institute of Marine Sciences, Kiel, Germany
[4]SRON Netherlands Institute for Space Research, Utrecht, The Netherlands
*now at: Department of Meteorology, University of Reading, UK
**now at: Shell International Exploration and Production B.V., Rijswijk, The Netherlands

Abstract. The relation between the Agulhas Current retroflection location and the magnitude of Agulhas leakage, the transport of water from the Indian to the Atlantic Ocean, is investigated in a high-resolution numerical ocean model. Sudden eastward retreats of the Agulhas Current retroflection loop are linearly related to the shedding of Agulhas rings, where larger retreats generate larger rings. Using numerical Lagrangian floats a 37 year time series of the magnitude of Agulhas leakage in the model is constructed. The time series exhibits large amounts of variability, both on weekly and annual time scales. A linear relation is found between the magnitude of Agulhas leakage and the location of the Agulhas Current retroflection, both binned to three month averages. In the relation, a more westward location of the Agulhas Current retroflection corresponds to an increased transport from the Indian Ocean to the Atlantic Ocean. When this relation is used in a linear regression and applied to almost 20 years of altimetry data, it yields a best estimate of the mean magnitude of Agulhas leakage of 13.2 Sv. The early retroflection of 2000, when Agulhas leakage was probably halved, can be identified using the regression.

1 Introduction

The Agulhas region, the region southeast and south of Africa where the Indian Ocean and Atlantic Ocean meet, plays a key role in the warm upper-branch return flow of the Atlantic meridional overturning circulation (Gordon, 1986; Weijer et al., 1999; Peeters et al., 2004; Biastoch et al., 2008a). The southward flowing Agulhas Current is the western boundary current of the Indian Ocean subtropical gyre. After separating from the continental slope near the southern tip of Africa, it flows southwestward until approximately 19° E, at which point it turns back into the Indian Ocean as the Agulhas Return Current (Lutjeharms and Van Ballegooyen, 1988). In this so-called retroflection loop, 4–6 Agulhas rings are shed per year. These anticyclones have diameters up to 300 km and form the main transport agent of thermocline water from the Indian Ocean to the Atlantic Ocean (e.g. De Ruijter et al., 1999; Lutjeharms, 2006).

The total volume flux of the Agulhas Current at 32° S is on the order of 70 Sv (Bryden et al., 2005). The bulk of this flux is recirculated in the subtropical gyre of the Indian Ocean, and only an estimated 5–15 Sv gets into the Atlantic Ocean as Agulhas leakage (Gordon et al., 1992; De Ruijter et al., 1999; Reason et al., 2003). Agulhas leakage is defined here as the water that is transported in the Agulhas Current and flows from the Indian Ocean into the Atlantic Ocean.

Estimating the magnitude of Agulhas leakage has proven to be difficult both in models and reality. This is in part because of the vigorous mixing in the Cape Basin, the area southwest of the African continent. Because coherent structures entering this basin are often quickly destroyed, Boebel et al. (2003a) dubbed the region the "Cape Cauldron". One way to estimate the magnitude of Agulhas leakage is to integrate the velocity as a function of depth and distance from the African coast. The problem with this Eulerian method,

however, is that the Cape Basin is not only drained from the Indian Ocean, but also from the Atlantic Ocean and the Southern Ocean. When estimating the magnitude of Agulhas leakage, these three sources of Cape Basin water have to be disentangled. Due to the turbulent nature of the flow in the Cape Basin and the resulting mixing, identifying separate water masses might be complicated, which is a main drawback of Eulerian velocity-based transport estimates.

An example of an Eulerian approach to estimating of the magnitude of Agulhas leakage is the Benguela Sources and Transports (BEST) experiment (e.g. Garzoli and Gordon, 1996), where Inverted Echo Sounder data is assimilated in a two-layer geostrophic model. The resulting transport time series has been combined with altimetry data by Goni et al. (1997) and Garzoli and Goni (2000) to yield a method to derive geostrophic baroclinic transports from altimetry data alone. The mean transport of 4 Sv obtained in this way is low compared to other estimates. Moreover, the authors admit that they have problems distinguishing Agulhas leakage from other sources of transport.

Dijkstra and De Ruijter (2001) have proposed an Eulerian retroflection index for the magnitude of Agulhas leakage, applied also by Hermes et al. (2007). Their index is based on the ratio between Agulhas Current inflow and Agulhas Return Current outflow as determined by volumetric fluxes of three-dimensional velocity fields from a numerical ocean model. Although powerful in models, this index can not be used in the real ocean where three-dimensional velocity field data sets are not available. Moreover, it is generally not easy to separate the Agulhas Return Current flow, which had its origin in the Agulhas Current, from other eastward flowing water masses such as the Antarctic Circumpolar Current. This makes the retroflection index sensitive to latitudinal shifts in the Southern Ocean frontal system near the Agulhas Return Current.

Because of the problems of mixed water masses, the Lagrangian volume transport might be a more appropriate measure of the magnitude of Agulhas leakage in a numerical model. Employing the trajectories of Lagrangian floats is an unambiguous and exact way to assess how much of the interocean flux originated in the Indian Ocean (Speich et al., 2006; Biastoch et al., 2008b). The drawback of using Lagrangian fluxes, however, is that these too are unavailable in the real ocean.

Currently, only altimeter products provide sustained observations of the ocean state in the Agulhas region. Sea surface height time series are available on high-resolution time scales and for almost 20 years. In this study, therefore, we relate the float-determined Agulhas leakage transport to information from modeled sea surface height, with the purpose to find the expression of Agulhas leakage at the sea surface. The location of the Agulhas Current western front is used as a proxy for ring shedding events and the amount of Agulhas leakage (Ou and De Ruijter, 1986; Lutjeharms and Van Ballegooyen, 1988; Feron et al., 1992).

In this study, results from a 1/10° numerical ocean model (Biastoch et al., 2008a,b) are used to retrieve a linear relation between the magnitude of Agulhas leakage and the most western longitude of the Agulhas Current retroflection loop. The method of finding the westward extent of the Agulhas Current retroflection and the numerical ocean model are introduced in Sect. 2. In Sect. 3, we find a linear relation between the speed of the eastward retreat in the Agulhas Current retroflection and the surface area of shedded Agulhas rings. The procedure for determining the magnitude of Agulhas leakage, using numerical Lagrangian floats, is described in Sect. 4. In Sect. 5, the westward extent of the Agulhas Current retroflection is related to the magnitude of Agulhas leakage to yield a linear estimate of leakage. In Sect. 6, then, the linear estimate is applied to altimetry data. This yields a first order estimate of the magnitude of Agulhas leakage and can be used to quantify early retroflections from altimetry. The articles ends with conclusions and discussion in Sect. 7.
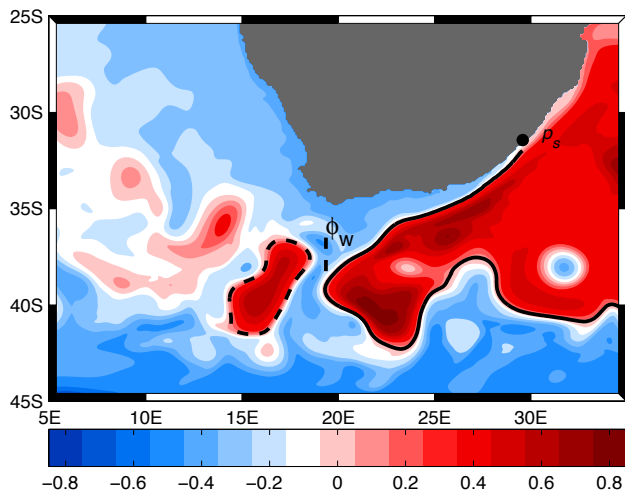
2 Tracking the Agulhas Current

Isolines of (model) sea surface height have been used before to track the location of the Agulhas Current (e.g Lutjeharms and Van Ballegooyen, 1988; Boebel et al., 2003b). In this study, the position of the Agulhas Current path is tracked by the following algorithm. From the sea surface height $h(\phi,\theta)$, geostrophic velocities $\boldsymbol{v}_g(\phi,\theta)$ are calculated. Using geostrophic velocity from sea surface height instead of model velocity fields has the advantage that the algorithm can also be applied to data sets where absolute velocity is unavailable, such as altimetry.

At 32° S, the grid cell $\boldsymbol{p_s}$ with highest southwestward geostrophic velocity is selected (Fig. 1). A counterclockwise contour $C_A(\phi,\theta)$ is drawn along all grid cells with height equal to $h(\boldsymbol{p_s})$. C_A extends to $\boldsymbol{p_e}$, the grid cell where the geostrophic velocity falls below a threshold value of $0.4|\boldsymbol{v}_g(\boldsymbol{p_s})|$. This value is chosen so that $\boldsymbol{p_e}$ is typically located east of 50° E. C_A resembles a proper retroflection when three additional conditions are satisfied: $\boldsymbol{p_e}$ should be east of $\boldsymbol{p_s}$, C_A should extent south of 37° S, and C_A should not close onto itself.

From the Agulhas Current contour $C_A(\phi,\theta)$ a proxy is formed. The variability of the Agulhas Current retroflection is best observed in its longitudinal location (Lutjeharms and Van Ballegooyen, 1988), so the westward extent of the Agulhas Current might serve as an appropriate proxy. In Fig. 1 this longitude is denoted as ϕ_w, which is defined as

$$\phi_w = \min_{\phi}\big(C_A(\phi,\theta)\big) \tag{1}$$

The algorithm is applied to the 1/10° AG01 model (Fig. 2) (Biastoch et al., 2008a,b). The model grid covers the greater Agulhas region (20° W–70° E; 47° S–7° S), nested into the ORCA model. The latter is a global ocean–sea-ice model on 1/2° grid. Both models are based on the NEMO code

Fig. 1. A snapshot of dynamic topography (in meter) on 20 November 2002 from the AG01 model. The thick black line is the Agulhas Current path C_A, starting at point p_s, as detected by the algorithm. The dashed closed contour is the associated ring found by the ring detection algorithm. The westward extent of the current is indicated by ϕ_w.

Fig. 2. Mean sea surface height (in meter) for a subregion of the AG01 model. The thick black line in the Atlantic Ocean denotes the location of the GoodHope line, over which the Agulhas leakage transport from numerical Lagrangian floats is determined.

(Madec, 2006, version 2.3). The nesting approach is two-way (Debreu et al., 2008), allowing the high-resolution AG01 nest to receive its open boundary values from the ORCA base model and to update the base model with data from the nest, thereby embedding the Agulhas system into the large-scale circulation. Both models have 46 vertical layers, with layer thicknesses ranging from 6 m at the surface to 250 m at depth, and employ partial cells at the ocean floor for a better representation of bathymetry. The two models are forced with the CORE data set of daily wind and surface forcing fields (Large and Yeager, 2004) for the period 1958–2004. The model output is available as the average of five day intervals. It was demonstrated that the mesoscale dynamics reflected in the decadal variability of the Atlantic meridional overturning circulation (Biastoch et al., 2008a).

Biastoch et al. (2008b) have demonstrated that the high-resolution nest captures the transport and currents of all components of the greater Agulhas system with substantial success, including perturbations in the Mozambique Channel and east of Madagascar. The data set comprises model output over the period 1968–2004 and the algorithm for tracking C_A succeeds in 99% of the snapshots.

The 1% of the snapshots where no proper contour can be detected seem to be related to events when extremely intense Natal pulses (Lutjeharms and Roberts, 1988) pass at 32° S. At some of these occasions the Agulhas Current temporarily meanders offshore so much that it can not be tracked any-more (although on most snapshots with a Natal pulse at 32° S the algorithm does not fail in finding a proper contour). Note that this does not necessarily mean that there is a bias in the ϕ_w data set, as it takes the Natal pulses a few months to
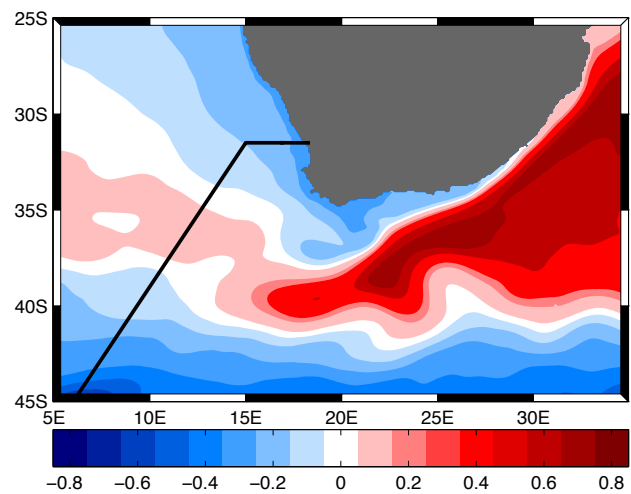
reach the Agulhas Current retroflection and possibly affect the westward extent (Van Leeuwen et al., 2000). This lag will assure that the moment of Natal pulse crossing at 32° S is uncorrelated to ϕ_w.

3 Relating the retroflection front retreat to ring size

In the sea surface height field, Agulhas rings are the most notable transport agent of Agulhas leakage (see also Van Sebille et al., 2009c). Although it is difficult to track the paths of these rings in noisy sea surface height data, ring shedding events themselves can more easily be detected. Several descriptions of the ring shedding mechanism have been proposed. In one of these (Ou and De Ruijter, 1986; Lutjeharms and Van Ballegooyen, 1988; Feron et al., 1992), the essential component is that the western front of the Agulhas Current slowly moves westward most of the time. At some moment, the loop formed by the Agulhas Current and Return Current occludes, an Agulhas ring pinches off, and the western front experiences an instantaneous eastward retreat.

The model time series shows evidence for the retroflection loop occlusion (Fig. 3). The histogram of the change in westward extent, $\Delta\phi_w/\Delta t$ is skewed, with a large peak at slower westward speeds and a smaller peak at higher eastward speeds (not shown). This is an indication for saw-tooth behavior, where the current retreat is quick as a ring sheds off, and the current progradation is slow as the Agulhas Current retroflection moves west.

Using $\Delta\phi_w/\Delta t$, ring shedding events can be detected. Whenever the Agulhas Current experiences a large retreat on the five day interval ($\Delta\phi_w/\Delta t > 0.4$ degree day^{-1}) this is considered a loop occlusion event and an associated ring is
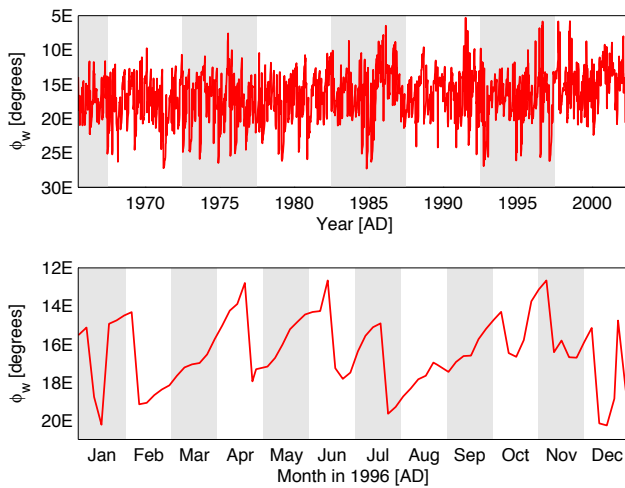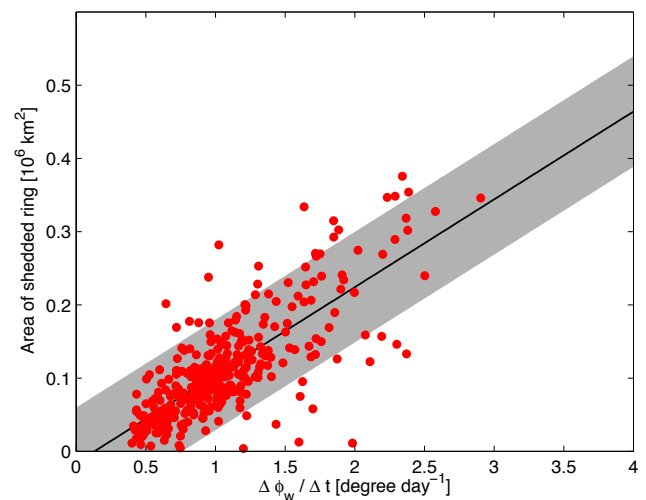
Fig. 3. Time series of the westward extent ϕ_w of the Agulhas Current for the AG01 model (upper panel) and a zoom of the westward extent ϕ_w for the year 1996 only (lower panel). The sawtooth behavior in the lower panel is an indication for the loop occlusion mechanism described by Lutjeharms and Van Ballegooyen (1988) and Feron et al. (1992). In this mechanism, a slow westward movement of the Agulhas Current front is followed by a fast eastward retreat as an Agulhas ring is pinched off.

Fig. 4. The change in front location for loop occlusion events for the AG01 model (when $\Delta\phi_w/\Delta t > 0.4$ degree day^{-1}) versus the area of the associated ring being shed. The black line is the best linear fit, with the gray area denoting the 90% confidence band. The correlation coefficient of the data set is 0.77.

sought in the dynamic height $h(\phi,\theta)$. An associated ring is defined as a closed contour of height equal to that of $C_A(\phi,\theta)$, located in a $1° \times 5°$ area west of ϕ_w (Fig. 1). Since it is close to ϕ_w, which has just experienced a sudden retreat, and has the same height as $C_A(\phi,\theta)$, we assume that the ring has just shed from the Agulhas Current. If a ring is found, the area inside the contour is taken as a measure of the ring size. If multiple closed contours are found, the one closest to ϕ_w is taken to be the associated ring. Since the Cape Basin is full of eddies, this happens regularly. In total, there are 37 occasions (11%) when one ring is found, 293 occasions (88%) when two or more rings are found, and 4 occasions (2%) when no rings are found.

There appears to be a relation in the model data between the magnitude of front retreat and ring size (Fig. 4). A larger retreat of the Agulhas Current retroflection results in a larger ring being shed. Note however, that this does not have to mean that the amount of Agulhas leakage is larger. Rings which have been shed are sometimes recaptured by the slowly westward protruding Agulhas Current. Therefore, the magnitude of Agulhas leakage can better be derived somewhat farther away from the retroflection, in the Cape Basin.

4 Measuring the Lagrangian Agulhas leakage transport

To quantify the possible relation between ϕ_w and the magnitude of Agulhas leakage, an assessment of the Agulhas leakage transport is made by tracking numerical floats. The float trajectories in the AG01 model are computed using the AR-

IANE package (Blanke and Raynaud, 1997), similar to the attempt by Biastoch et al. (2008b) to estimate the long-term statistics of the modeled interocean exchange. The isopycnal floats are released every five days throughout the water column at 32° S, depending on the instantaneous local volume flux (see Fig. 5). The initial transport per float is capped at 0.1 Sv, but a large portion of the floats represent a lower transport to allow for sampling in grid cells where transport is lower than 0.1 Sv. The floats are integrated for five years, so that most floats reach the domain boundaries. The total number of floats released in the model is $5.6 \cdot 10^6$, launched over a period of 37 years (1968–2004). After the five year integration period, only 3% of the numerical floats have not exited the domain. The mean model Agulhas Current transport at 32° S is 64 Sv.

Using the float data, a time series of the Agulhas leakage transport is constructed for the model. Only floats of which the final position is west of the GoodHope line (see Fig. 2) are taken into account. The GoodHope line (Swart et al., 2008) is a combined XBT and PIES line currently used to estimate Eulerian fluxes. Choosing this line facilitates future comparison between the Lagrangian fluxes presented here and in situ Eulerian estimations. Van Sebille et al. (2009b) have shown that the model used here might possess skill, in the sense that the statistical properties of the numerical float trajectories can not be considered very different from the statistical properties of the trajectories of real drifting buoys in the Agulhas area.

The transport of each float crossing the GoodHope line is added to the Agulhas leakage flux $F_{AL}(t)$, where t is the last time the float crosses the line. In this way, floats that cross
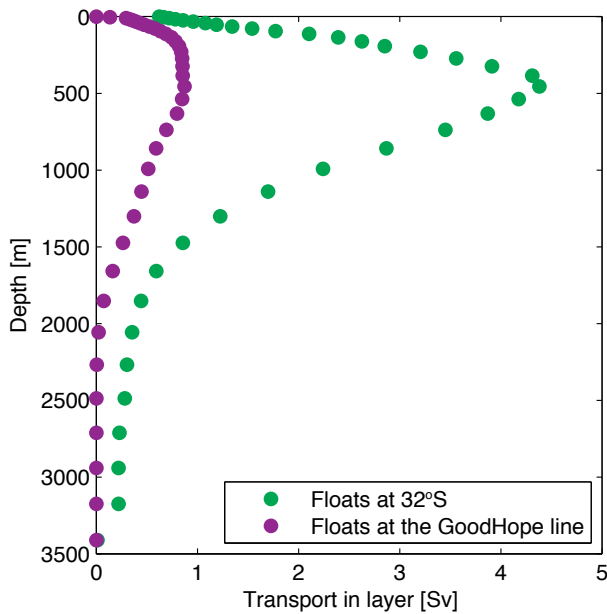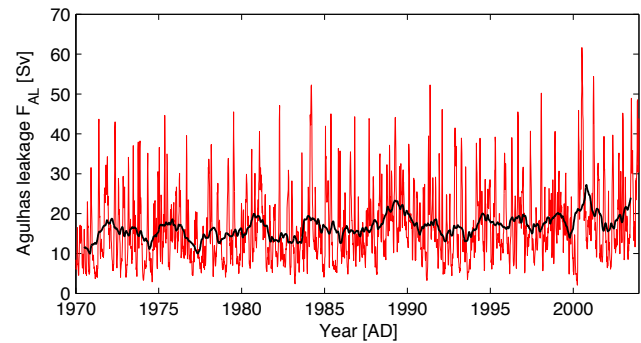
Fig. 5. Mean transport by the Lagrangian floats per model layer at the location where the floats are released (green) and when the floats get into the Altantic Ocean at the GoodHope line (purple). The isopycnal floats are seeded according to local volume flux, so most floats are seeded in the upper 1500 m. The transport at 32° S by floats seeded below 2000 m is 1.62 Sv, but the transport across the GoodHope line by these deep floats is only 0.03 Sv.

Fig. 6. Time series of the Agulhas leakage transport F_{AL}, the flux of water sampled by the numerical floats over the GoodHope line in red, and the one year smoothed time series in black. The mean magnitude of Agulhas leakage is 16.7 Sv, with a standard deviation of 9.2 Sv. The Agulhas leakage transport never gets to zero on this five day resolution.

the line several times are only added to the Agulhas leakage flux time series once, at the moment of their last crossing if that is into the Atlantic Ocean. The flux from floats that cross the GoodHope line and end in the Indian Ocean is negligible.

The estimates of the magnitude of Agulhas leakage in literature have a large range, from 4 Sv (Schmitz Jr, 1995; Garzoli and Gordon, 1996) to 22 Sv (Donners and Drijfhout, 2004). However, most studies report an estimate of 11–17 Sv. These estimates are based on different methods, such as water mass analysis (Gordon et al., 1992), altimetry (Garzoli and Goni, 2000), Eulerian model fluxes (Reason et al., 2003), numerical Lagrangian floats (Doglioli et al., 2006; Biastoch et al., 2008b), or drifting buoy trajectories (Richardson, 2007). However, none of these studies provide an estimate of the (interannual) variability of Agulhas leakage as the time series obtained in these measurement campaigns or model runs is generally too short to yield higher order statistics.

The 37 year long time series in the AG01 model allows for an estimation of the variability of the modeled Agulhas leakage transport. The average leakage in the model is 16.7 Sv, with a variability of 9.2 Sv (Fig. 6). When a one year moving average window is applied to smooth the Agulhas leakage transport time series, there is clear interannual variability, with Agulhas leakage transports ranging between 10 and 25 Sv.

There is a 0.18 Sv/year linear trend in the time series. This is probably related to a 20% decrease in wind stress curl over the Indian Ocean in the period 1968–2002 in the Large and Yeager (2004) data set. This decrease in wind stress curl may cause a weaker Indian Ocean subtropical gyre, and hence a weaker Agulhas Current. As there is an anticorrelation between Agulhas Current strength and the magnitude of Agulhas leakage (Van Sebille et al., 2009a), the reduced wind stress curl would imply an enhanced leakage. In the model, indeed, there is a negative trend in the amount of floats being seeded but a positive trend in the amount of floats that end up in the Atlantic Ocean.

The mean leakage over a five day period can peak at more than 50 Sv. This is the case when an Agulhas ring passes through the section, and a large bulk of Agulhas Current water is advected over the GoodHope line. The leakage never goes to zero, so there is always some small background leakage on the five day resolution used here.

There is almost no Agulhas leakage below 2000 m, although there are floats which are released deeper in the Agulhas Current (Fig. 5). Apparently, only the upper part of the Agulhas Current leaks into the Atlantic Ocean and the lower part is returned into the Indian Ocean in this model. The relative shallowness of Agulhas leakage was also found by Donners et al. (2004), who reported that Agulhas leakage was limited to the upper 1200 m in their model. Furthermore, using observations, Van Aken et al. (2003) show that an Agulhas ring has low relative vorticity below 1200 m, which might imply that deeper than 1200 m there is almost no mass carried by the rings. In a model study, De Steur et al. (2004) showed that the size of the seperatrix (the circumference of the region where water is advected with an Agulhas ring) decreases with depth due to the decrease in swirl velocity of the water. At some depth, therefore, the swirl velocity is smaller than the translational velocity, and the Agulhas rings can not advect water anymore (Flierl, 1981).

Since the float positions are available on five day resolution only, the calculation of crossing positions at the Good-Hope line introduces at least three kinds of errors. First of all, by using five day means, some of the small-scale features of the Agulhas leakage may be smeared out and not correctly sampled. A second error may be introduced since the trajectories are computed using velocity fields which are updated only every five days. During the time steps following the update the velocity fields do not change. Note that this error might be reduced with a float integration scheme that linearly interpolates the velocity fields between the five day means (De Vries and Döös, 2001). Finally, an error may be introduced since the float intersections with the GoodHope line are calculated by a linear mapping onto the GoodHope line, but the float trajectories are certainly not straight between consecutive model averages.

The error in GoodHope line crossing position can be investigated by testing the modeled Agulhas leakage transport dependency on the temporal resolution. For the year 1980, an experiment was done where numerical floats were advected using one day averaged model fields. The trajectories in this experiment are not more than one year long. The float crossings at the GoodHope line in this experiment can be compared to the float crossings in the experiment on five day resolution (Fig. 7). The agreement between the crossings is high, both in spacing ($R = 0.95$) and timing ($R = 0.97$).

The only major discrepancy between the two experiments is found in the crossing locations through the GoodHope line, where the relative void in float crossings at 750 km offshore is much deeper in the one day resolution experiment than it is in the five day resolution experiment. The bipartitioning seems to be related to the peak in transport over the Good-Hope line around day 275, as it disappears when the float data set is reduced to only crossings in the first 200 days of 1980 (not shown). But apart from this feature, reducing the float integration to five day resolution does not seem to affect the float crossings at the GoodHope line.

The good agreement between the location of the floats and dynamical structures can also be observed in snapshots of the float distribution with the five-day mean sea surface height field overlayed (Fig. 8). On any given moment, there are in the order of 10^6 floats in the domain, so there are almost no areas which are void of floats (except for areas of pure Atlantic Ocean or Southern Ocean water, mainly in the Antarctic Circumpolar Current). However, there is a clear tendency for floats to cluster in Agulhas rings and Agulhas cyclones, especially close to the retroflection region. Further into the Atlantic Ocean, the distribution is more homogeneous. This decay of Agulhas rings and the consequences for the fate of Agulhas leakage is further discussed in Van Sebille et al. (2009c).
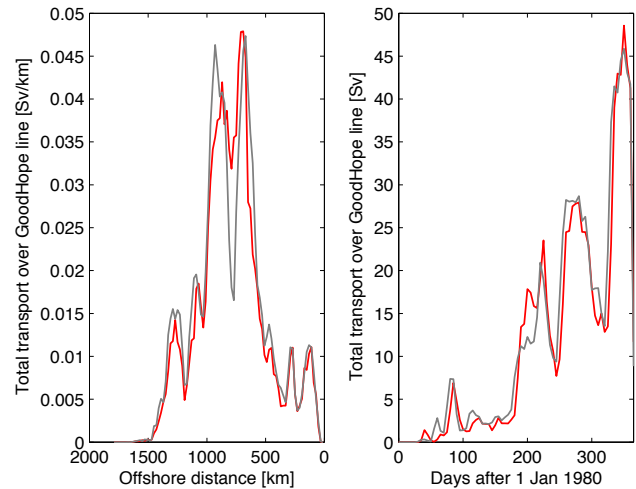
Fig. 7. Float-determined transport over the GoodHope line for the default model run using five day averaged model fields (red lines), and a short run using one-day averaged model fields (gray lines). Only float trajectories starting in 1980 are used. The transport as a function of offshore distance (left panel) and the transport over the GoodHope line as a function of time (right panel) are shown. Apart from a decreased transport in the one-day averaged model fields at 750 km offshore, the transport variability is quite similar, both in space and time.
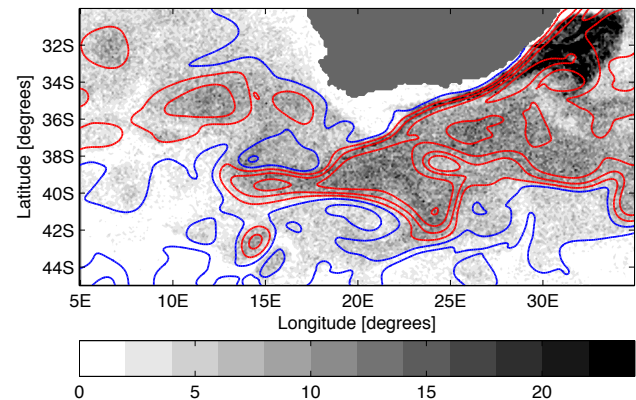
Fig. 8. The number of floats per grid cell in the model run on 20 April 1996. In total, there are $2.3 \cdot 10^6$ floats in this subdomain of the high-resolution nested model. The lines denote the instantaneous sea surface height (at a contour interval of 25 cm), with negative values in blue and positive values in red. This snapshot is typical for the model, where there is a high correlation between sea surface height information (Agulhas rings, eddies, fronts) and the density of Lagrangian floats.

5 Relating Agulhas leakage to sea surface height

Both the modeled westward extent ϕ_w and the modeled Agulhas leakage transport F_{AL} are highly variable, which is due to the intermittent nature of the shedding of Agulhas rings (Fig. 3 and Fig. 6). The crosscorrelation between these two

quantities is maximum at a lag of 105 days. Such a lag agrees roughly with the time it takes the Agulhas rings to drift from the location where they are shed to the GoodHope line, a distance of approximately 500 km (from 17.5° E to 12° E). Byrne et al. (1995) and Schouten et al. (2000) found an Agulhas ring translation speed in this region of 5 km/day, which leads to a comparable translation time (100 days).

Since the amount of noise in the area is high the time series are subsampled to three month bins. We choose a 95 day low-pass filter, as it yields the best signal-to-noise ratio: a high crosscorrelation level between T_{AL} and Φ_w on the one hand, and a low crosscorrelation significance level on the other. Given the chaotic nature of the fluid flow in the retroflection area and the continuous motion of the front, one would expect a time scale related to the shedding frequency of the rings (90 days for four rings per year), or longer if longer time scales exist in the system. For larger averaging periods, however, the time series is too short and thus the crosscorrelation significance level is too high. These considerations lead to the following definition of the westward extent and Agulhas leakage transport:

$$\Phi_w(t) = \langle \phi_w(t - 105 \text{ days}) \rangle \qquad T_{AL}(t) = \langle F_{AL}(t) \rangle \qquad (2)$$

where $\langle \ldots \rangle$ is the 95 day binning operator.

The correlation between the time series of Φ_w and T_{AL} is -0.48, which is significantly different from zero at the 90% confidence level (Fig. 9). This correlation is not very high, which is also evident from the large spread in data points, but it supports our hypothesis that in the model a more westward location of the Agulhas Current retroflection leads to an increase in the magnitude of Agulhas leakage.

From a dynamical perspective, the possible relation between westward extent and leakage could be explained by two mechanisms. First of all, a westward zonal jet is more unstable than an eastward one (Gill et al., 1974), so that, if Φ_w is more westward, the potential for instabilities to grow and rings to pinch off is larger. Secondly, a more westward retroflection causes the eddies to be spawned farther into the Atlantic Ocean, where they have a lower chance of being re-entrained into the Agulhas Current (Pichevin et al., 2009).

To quantify the relation between retroflection location and leakage, a linear regression has been performed on the data points. This leads to a linear estimate of the magnitude of Agulhas leakage E_{AL}, given the 95 day binned westward extent:

$$E_{AL} = \alpha \ \Phi_w + \beta \qquad (3)$$

where the fitting parameters $\alpha = -1.1$ Sv/degree and $\beta = 36.1$ Sv are obtained from the best fit of the 95 day means in Fig. 9.

Due to the relatively low correlation between Φ_w and T_{AL}, the skill of the linear estimate is not very high. This can be quantified by assigning a confidence band to the linear estimate. As a first approximation, a constant band is chosen
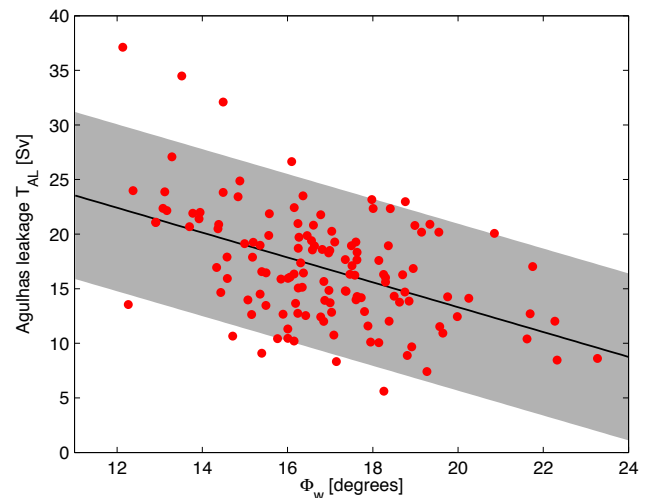

Fig. 9. The 95 day binned float-determined Agulhas leakage transport T_{AL} versus westward extent Φ_w for the model data. The black line is the best linear fit and the gray area indicates the estimated confidence band so that 90% of the data points fall within the area. The correlation between the two data sets is -0.48, which is significant at the 90% confidence level.

such that 90% of the data points lie within that band. This 90% confidence band results in an uncertainty of 15 Sv in the estimate. An estimate of the magnitude of Agulhas leakage based on the current's westward extent is therefore only certain within a 15 Sv range and this might limit the usability of the quantitative relation Eq. (3). However, the observation that there is a significant linear relation is more robust (see also the discussion, Sect. 7). Further note that the one standard deviation error estimate is much lower, at 5.4 Sv.

6 Application to altimetry data

The relation which has been found in the previous section can be used to construct an estimate of the magnitude of Agulhas leakage when only sea surface height data are available. The algorithm for finding ϕ_w as described in Sect. 2 was designed to be also applicable to altimetry data, since geostrophic velocities are used instead of model velocities. Applying the linear estimate of Eq. (3) to altimetry data, where the true magnitude of Agulhas leakage is unknown, might yield some first estimate of the mean and variability of the magnitude of Agulhas leakage in the real ocean.

The altimetry data used is from the AVISO project: more than 15 years of weekly merged sea level anomalies in the Agulhas region on a 1/4° resolution, combined with the Rio and Hernandez (2004) mean dynamic topography. The algorithm for tracking the Agulhas Current detects a contour C_A in 94% of the snapshots. The mean westward extent in the data set is 19.3° E.
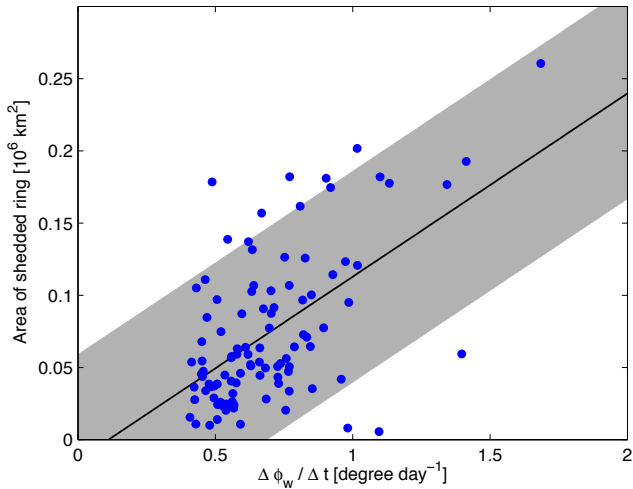
Fig. 10. The change in front location for loop occlusion events for the AVISO altimetry data (when $\Delta\phi_w/\Delta t > 0.4$ degree day^{-1}) versus the area of the associated ring being shed. The gray area denotes the 90% confidence band. The correlation coefficient of the data set is 0.59. Although the spread in data points is smaller than in the AG01 model (Fig. 4, note the different scales of the axes), both the linear relation and the width of the 90% confidence band are similar.

The variability in westward extent is much smaller in the AVISO altimetry data set than in the AG01 model data set. The magnitude of large ring retreats is generally smaller (compare Fig. 10 with Fig. 4). Nevertheless, the relation between front retreat and area of the shedded ring is similar, with the best linear fit having almost the same slope (both $1.2 \cdot 10^5$ km^2 day degree^{-1}). Furthermore, the distribution of the amount of rings in the $1° \times 5°$ area just west of ϕ_w is also very comparable, at 14% of the snapshots with one ring in the area (11% in the model), 86% with two or more rings (88% in the model), and 0% with no rings (2% in the model). This correspondence of both slope and amount of rings between model and altimetry is a somewhat surprising validation of the AG01 model.

The linear estimate of Eq. (3) yields an estimated time series E_{AL} for the AVISO altimetry (Fig. 11). The mean magnitude of Agulhas leakage in the AVISO data set is 13.2 Sv, with a variability of 1.5 Sv. The most prominent feature in the time series is the drop in the magnitude of Agulhas leakage in the beginning of 2001. This drop coincides with the early retroflection of December 2000 (De Ruijter et al., 2004). In this period, the Agulhas Current retroflected east of the Agulhas Plateau for almost six months, and no Agulhas rings were formed. Such early retroflections are important large-scale events. One more has been reported, by Shannon et al. (1990) in 1986. The AG01 model also has early retroflections, but these seem to be a bit too common (Biastoch et al., 2008b).
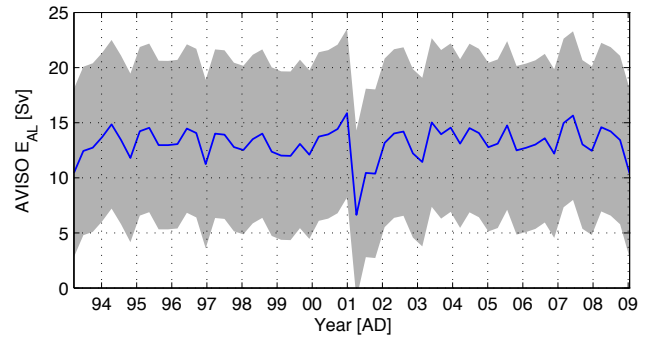
Fig. 11. The estimated magnitude of Agulhas leakage from E_{AL} (gray area as 90% confidence band) for the 95 day binned AVISO altimetry data. The sharp decrease of E_{AL} in 2001 coincides with an early retroflection (De Ruijter et al., 2004). According to the estimate, it is very likely that during this early retroflection the magnitude of Agulhas leakage was reduced.

The 15 Sv confidence band around the linear estimate of the magnitude of Agulhas leakage in the AVISO data seems to prohibit any more detailed analysis of the time series. But this is only true for the analysis on the magnitude of Agulhas leakage, which is computed using information from the data points in Fig. 9. The variability in the magnitude of Agulhas leakage, on the other hand, is directly related to the variability in westward extent Φ_w and may therefore be analyzed. Although it is not significant, there seems to be evidence for an annual cycle in the westward extent of the Agulhas Current retroflection in the AVISO data, with a more westward Agulhas Current retroflection in austral winter.

The much lower variability in the AVISO data set than in the AG01 data sets appears to be related to the relatively high fraction of the time that the Agulhas Current retroflection is west of 15° E in the model (Fig. 12). On the original temporal resolution of the model (five days) and the altimetry data (seven days), the distributions of the eastward tails (the early retroflections) of ϕ_w are similar. West of 23° E, however, the model has a much wider spread in its distribution of ϕ_w than the altimetry data. The spread is closely related to the Agulhas leakage variability, through the linear relation. An explanation for this wide band of ϕ_w may be in details of the numerical representation such as viscosity parameterizations and used values. The wider distribution is in agreement with the more westward flowing Agulhas Current and the associated larger ring area in the model compared to the altimetry data (compare Fig. 4 with Fig. 10).

7 Conclusions and discussion

The influence of the westward extent of the Agulhas Current on the magnitude of Agulhas leakage has been investigated by releasing floats in the high-resolution two-way nested AG01 numerical ocean model. A relation has been
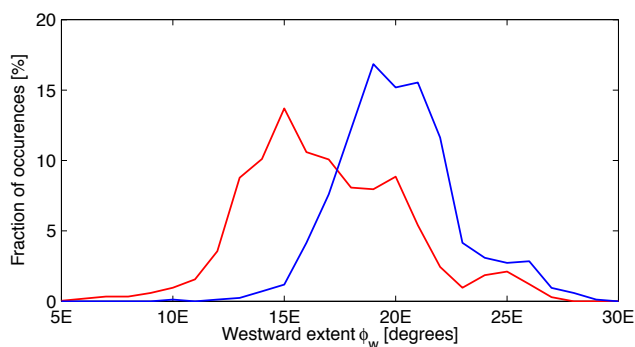
Fig. 12. Distributions of the non-smoothed westward extent of the Agulhas Current retroflection ϕ_w for the AG01 model data (red line) and the AVISO altimetry data (blue line). For high values of the westward extent (early retroflections, $\phi_w > 23°$ E) the distributions of the two data sets are similar, but the low ϕ_w tail in the model data is much more westward than for the altimetry data. This explains the relatively low variability in AVISO E_{AL} compared to the variability in AG01 data (Fig. 11). The wider distribution, especially on the low ϕ_w tail, of the model data is also related to the larger rings that are shed in the model (compare Fig. 4 with Fig. 10).

found between speed of current retreat and the size of the shed ring, which supports the loop occlusion mechanism of ring shedding (Ou and De Ruijter, 1986; Lutjeharms and Van Ballegooyen, 1988; Feron et al., 1992). Moreover, a correlation ($R = -0.48$, which is significant at the 90% confidence level) between the 95 day binned Agulhas Current retroflection front location and the 95 day binned magnitude of Agulhas leakage has been found. This correlation implies that a more westward Agulhas Current retroflection leads to enhanced Agulhas leakage transports. A linear estimate for the magnitude of Agulhas leakage can be constructed based on the correlation for use when only sea surface height information is available.

The linear estimate E_{AL} of Eq. (3) has a 15 Sv confidence band around the best estimate. This means that application of the estimate leads to an amount of Agulhas leakage which is 90% certain in a 15 Sv range. Such a range is generally too large to be useful, as is demonstrated in the application to the AVISO data set (Fig. 11). The aptness of the linear estimate to serve as an index to quantify variability in the amount of Agulhas leakage is therefore limited.

In contrast, the linear relation between the westward extent of the Agulhas Current retroflection and the magnitude of Agulhas leakage is significant. This study might therefore be of more use in increasing the understanding of the Agulhas system dynamics than in providing a way to estimate the magnitude of Agulhas leakage. Nevertheless, the robustness of the linear relation might mean that the confidence band can be reduced by increasing the size of the data sets. In the future it might be possible to construct a usable index based on the westward extent of the Agulhas Current retroflection.

A fundamental assumption in the linear relation between Φ_w and T_{AL} is that, by monitoring the Agulhas Current location, we can make a good assessment of the total magnitude of Agulhas leakage, which includes small-scale features such as filaments (Lutjeharms and Cooper, 1996; Treguier et al., 2003; Doglioli et al., 2006). While these features are not captured in the front movement, they are sampled by the numerical floats. Therefore, the relation found for estimating the magnitude of Agulhas leakage accounts for all leakage, including that of small-scale filaments.

The transport estimate in the AVISO data set in only slightly lower than estimated from direct observations and the 2001 early retroflection is unambiguously captured by the altimeter data. However, the validity of these results is limited as the relation between Agulhas Current location and the magnitude of Agulhas leakage is derived from model data only, and no verification with in situ observation has been done. The ultimate relation should come from an absolute estimate of the magnitude of Agulhas leakage from observational programs, where interocean fluxes are directly measured.

References

Biastoch, A., Böning, C. W., and Lutjeharms, J. R. E.: Agulhas leakage dynamics affects decadal variability in Atlantic overturning circulation, Nature, 456, 489–492, 2008a.

Biastoch, A., Lutjeharms, J. R. E., Böning, C. W., and Scheinert, M.: Mesoscale perturbations control inter-ocean exchange south of Africa, Geophys. Res. Lett., 35, L20602, doi:10.1029/2008GL035132, 2008b.

Blanke, B. and Raynaud, S.: Kinematics of the Pacific Equatorial Undercurrent: An Eulerian and Lagrangian approach from GCM results, J. Phys. Oceanogr., 27, 1038–1053, 1997.

Boebel, O., Lutjeharms, J. R. E., Schmid, C., Zenk, W., Rossby, T., and Barron, C. N.: The Cape Cauldron, a regime of turbulent inter-ocean exchange, Deep Sea Res. II, 50, 57–86, 2003a.

Boebel, O., Rossby, T., Lutjeharms, J. R. E., Zenk, W., and Barron, C. N.: Path and Variability of the Agulhas Return Current, Deep Sea Res. II, 50, 35–56, 2003b.

Bryden, H. L., Beal, L. M., and Duncan, L. M.: Structure and Transport of the Agulhas Current and Its Temporal Variability, J. Oceanogr., 61, 479–492, 2005.

Byrne, D. A., Gordon, A. L., and Haxby, W. F.: Agulhas Eddies: A synoptic View Using Geosat ERM Data, J. Phys. Oceanogr., 25, 902–917, 1995.

De Ruijter, W. P. M., Biastoch, A., Drijfhout, S. S., Lutjeharms, J. R. E., Matano, R. P., Pichevin, T., Van Leeuwen, P. J., and Weijer, W.: Indian-Atlantic interocean exchange: dynamics, estimation, and impact, J. Geophys. Res., 104, 20885–20910, 1999.

De Ruijter, W. P. M., Van Aken, H. M., Beier, E. J., Lutjeharms, J. R. E., Matano, R. P., and Schouten, M. W.: Eddies and dipoles around South Madagascar: formation, pathways and large-scale impact, Deep Sea Res. I, 53, 383–400, 2004.

De Steur, L., Van Leeuwen, P. J., and Drijfhout, S. S.: Tracer leakage from modeled Agulhas rings, J. Phys. Oceanogr., 34, 1387–1399, 2004.

De Vries, P. and Döös, K.: Calculating Lagrangian Trajectories Using Time-Dependent Velocity Fields, J. Atmos. Ocean. Tech., 18, 1092–1101, 2001.

Debreu, L., Vouland, C., and Blayo, E.: AGRIF: Adaptive grid refinement in Fortran, Comput. Geosci., 34, 8–13, 2008.

Dijkstra, H. A. and De Ruijter, W. P. M.: On the physics of the Agulhas current: steady retroflection regimes, J. Phys. Oceanogr., 31, 2971–2985, 2001.

Doglioli, A. M., Veneziani, M., Blanke, B., Speich, S., and Griffa, A.: A Lagrangian analysis of the Indian-Atlantic interocean exchange in a regional model, Geophys. Res. Lett., 33, L14611, doi:10.1029/2006GL026498, 2006.

Donners, J. and Drijfhout, S. S.: The Lagrangian view of South Atlantic interocean exchange in a global ocean model compared with inverse model results, J. Phys. Oceanogr., 34, 1019–1035, 2004.

Donners, J., Drijfhout, S. S., and Coward, A. C.: Impact of cooling on the water mass exchange of Agulhas rings in a high resolution ocean model, Geophys. Res. Lett., 31, L16312, doi:10.1029/2004GL020644, 2004.

Feron, R. C. V., De Ruijter, W. P. M., and Oskam, D.: Ring shedding in the Agulhas Current System, J. Geophys. Res., 97, 9467–9477, 1992.

Flierl, G. A.: Particle motions in large-amplitude wave fields, Geophys. Astrophys. Fluid Dynam., 18, 39–74, 1981.

Garzoli, S. L. and Goni, G. J.: Combining altimeter observations and oceanographic data for ocean circulations and climate studies, chap. 5, Elsevier Oceanographic Series, 79–97, 2000.

Garzoli, S. L. and Gordon, A. L.: Origins and variability of the Benguela Current, J. Geophys. Res., 101, 897–906, 1996.

Gill, A. E., Green, J. S. A., and Simmons, A. J.: Energy partition in the large-scale ocean circulation and the production of mid-ocean eddies, Deep Sea Res., 21, 499–528, 1974.

Goni, G. J., Garzoli, S. L., Roubicek, A. J., Olson, D. B., and Brown, O. B.: Agulhas ring dynamics from TOPEX/POSEIDON satellite altimeter data, J. Mar. Res., 55, 861–883, 1997.

Gordon, A. L.: Interocean Exchange of Thermocline Water, J. Geophys. Res., 91, 5037–5046, 1986.

Gordon, A. L., Weiss, R. F., Smethie Jr., W. M., and Warner, M. J.: Thermocline and intermediate water communication between the South Atlantic and Indian Oceans, J. Geophys. Res., 97, 7223–7240, 1992.

Hermes, J. C., Reason, C. J. C., and Lutjeharms, J. R. E.: Modeling the Variability of the Greater Agulhas Current System, J. Climate, 20, 3131–3146, 2007.

Large, W. G. and Yeager, S. G.: Diurnal to decadal global forcing for ocean and sea-ice models: the data sets and flux climatologies, NCAR Technical Note NCAR/TN-460+STR, NCAR, 2004.

Lutjeharms, J. R. E.: The Agulhas Current, Springer, Berlin, Germany, 329 pp., 2006.

Lutjeharms, J. R. E. and Cooper, J.: Interbasin leakage through Agulhas Current filaments, Deep Sea Res. I, 43, 213–238, 1996.

Lutjeharms, J. R. E. and Roberts, H. R.: The Natal Pulse: An extreme transient on the Agulhas Current, J. Geophys. Res., 93, 631–645, 1988.

Lutjeharms, J. R. E. and Van Ballegooyen, R. C.: The Retroflection of the Agulhas Current, J. Phys. Oceanogr., 18, 1570–1583, 1988.

Madec, G.: NEMO ocean engine, Note du pôle de modélisation, Institut Pierre-Simon Laplace (IPSL), 2006.

Ou, H. W. and De Ruijter, W. P. M.: Separation of an Inertial Boundary Current from a Curved Coastline, J. Phys. Oceanogr., 16, 280–289, 1986.

Peeters, F. J. C., Acheson, R., Brummer, G. A., De Ruijter, W. P. M., Schneider, R. R., Ganssen, G. M., Ufkes, E., and Kroon, D.: Vigorous exchange between the Indian and Atlantic oceans at the end of the past five glacial periods, Nature, 430, 661–665, 2004.

Pichevin, T., Herbette, S., and Floc'h, F.: Eddy formation and shedding in a separating boundary current, J. Phys. Oceanogr., 39, 1921–1934, 2009.

Reason, C. J. C., Lutjeharms, J. R. E., Hermes, J., Biastoch, A., and Roman, R. E.: Inter-ocean fluxes south of Africa in an eddy-permitting model, Deep Sea Res. II, 50, 281–298, 2003.

Richardson, P. L.: Agulhas leakage into the Atlantic estimated with subsurface floats and surface drifters, Deep Sea Res. I, 54, 1361–1389, 2007.

Rio, M. H. and Hernandez, F.: A mean dynamic topography computed over the world ocean from altimetry, in situ measurements, and a geoid model, J. Geophys. Res., 109, C12032, doi:10.1029/2003JC002226, 2004.

Schmitz Jr, W. J.: On the interbasin-scale thermohaline circulation, Rev. Geophys., 33, 151–173, 1995.

Schouten, M. W., De Ruijter, W. P. M., Van Leeuwen, P. J., and Lutjeharms, J. R. E.: Translation, decay and splitting of Agulhas rings in the southeastern Atlantic Ocean, J. Geophys. Res., 105, 21913–21925, 2000.

Shannon, L. V., Agenbag, J. J., Walker, N. D., and Lutjeharms, J. R. E.: A major pertubation in the Agulhas retroflection area in 1986, Deep Sea Res., 37, 493–512, 1990.

Speich, S., Lutjeharms, J. R. E., Penven, P., and Blanke, B.: Role of bathymetry in Agulhas Current configuration and behaviour, Geophys. Res. Lett., 33, L23611, doi:10.1029/200GL014586, 2006.

Swart, S., Speich, S., Ansorge, I. J., Goni, G. J., Gladyshev, S., and Lutjeharms, J. R. E.: Transport and variability of the Antarctic Circumpolar Current south of Africa, J. Geophys. Res., 113, C09014, doi:10.1029/2007JC004223, 2008.

Treguier, A. M., Boebel, O., Barnier, C., and Madec, G.: Agulhas eddy fluxes in a 1/6° Atlantic model, Deep Sea Res. II, 50, 251–280, 2003.

Van Aken, H. M., Van Veldhoven, A. K., Veth, C., De Ruijter, W. P. M., Van Leeuwen, P. J., Drijfhout, S. S., Whittle, C. C., and Rouault, M.: Observations of a young Agulhas ring, Astrid, during MARE in March 2000, Deep Sea Res. II, 50, 167–195, 2003.

Van Leeuwen, P. J., De Ruijter, W. P. M., and Lutjeharms, J. R. E.: Natal pulses and the formation of Agulhas rings, J. Geophys. Res., 105, 6425–6436, 2000.

Van Sebille, E., Biastoch, A., Van Leeuwen, P. J., and De Ruijter, W. P. M.: A weaker Agulhas Current leads to more Agulhas leakage, Geophys. Res. Lett., 36, L03601, doi:10.1029/2008GL036614, 2009a.

Van Sebille, E., Van Leeuwen, P. J., Biastoch, A., Barron, C. N., and De Ruijter, W. P. M.: Lagrangian validation of numerical drifter trajectories using drifting buoys: Application to the Agulhas region, Ocean Model., 29, 269–276, 2009b.

Van Sebille, E., Van Leeuwen, P. J., Biastoch, A., and De Ruijter, W. P. M.: On the fast decay of Agulhas rings, J. Geophys. Res., doi:10.1029/2009JC005585, in press, 2009c.

Weijer, W., De Ruijter, W. P. M., Dijkstra, H. A., and Van Leeuwen, P. J.: Impact of Interbasin Exchange on the Atlantic Overturning Circulation, J. Phys. Oceanogr., 29, 2266–2284, 1999.